

# Variation of Air-Water Gas Transfer with Wind Stress and Surface Viscoelasticity

Nelson M. Frew<sup>1</sup>, Erik J. Bock<sup>1</sup>, Wade R. McGillis<sup>1</sup>,  
Andrey V. Karachintsev<sup>1</sup>, Tetsu Hara<sup>2</sup>, Thomas Münsterer<sup>3</sup>,  
and Bernd Jähne<sup>3</sup>

<sup>1</sup> Woods Hole Oceanographic Institution (WHOI)

<sup>2</sup> Graduate School of Oceanography, University of Rhode Island

<sup>3</sup> Institute for Environmental Physics, University of Heidelberg (UH)

## Abstract

Previous parameterizations of gas transfer velocity have attempted to cast this quantity as a function of wind speed or wind-stress. This study demonstrates that the presence of a surface film is effective at reducing the gas transfer velocity at constant wind-stress. Gas exchange experiments were performed at WHOI and UH using annular wind-wave tanks of different scales. Systematic variations of wind-stress and surfactant concentration (Triton-X-100) were explored to determine their influence on gas transfer velocity. Attempts to characterize the surface properties of the surfactant solutions were performed using mechanically generated capillary-wave packets. Results indicate a strong inverse relationship between gas transfer velocity and enhanced wave damping.

## 1 Introduction

The exchange of gases by the oceans is an important component of global budgets for the cycling of climatically important gases, including carbon dioxide and other trace gases. Estimation of ocean-atmosphere gas fluxes requires a knowledge of gas concentration gradients and an accurate parameterization of the gas transfer velocity ( $k$ ). Previous studies of gas transfer have shown a strong dependence of the gas transfer velocity on wind and a weaker dependence on gas diffusivity [Jähne *et al.*, 1987]. Thus, the exchange velocity is commonly parameterized as a function of *wind speed* ( $u$ ) and *Schmidt number* ( $Sc$ ). Field estimates of  $k$  using natural and bomb <sup>14</sup>C inventories, radon and other gas tracers show considerable scatter as a function of wind, attributable in part to variable fetch, wave state and, owing to the nonlinearity of the  $u - k$  relation, biases introduced by the use of averaged winds [Wanninkhof, 1992]. Laboratory measurements carried out under tightly controlled conditions in wind-wave tanks also show large variations in  $k$  at constant or nearly constant friction velocity, suggesting that wind stress alone is not sufficient to parameterize  $k$ , and that other factors enter into the exchange process [Jähne *et al.*, 1987].

Recent observations suggest that surface-active materials present naturally in lakes and seas and also adventitiously in laboratory wind-wave tanks have a significant effect on the gas transfer velocity [Frew, 1995]. From studies in turbulent systems, it is known that *surface films* affect near-surface turbulence length and velocity scales [Lee *et al.*, 1980]. The viscoelastic modulus introduced by the presence of surfactants at the gas-liquid interface represents an additional tangential stress that opposes surface divergence due to turbulent eddies [Davies, 1966]. Thus, the presence of a film inhibits surface renewal and the resultant exchange of gases between the two phases.

Wind-generated waves transfer energy to turbulence via wave-wave interactions [Jähne *et al.*, 1987]. Thus, factors that modify the spectral characteristics of the wave field are likely to affect turbulence and the transfer process. The effect of finite *surface viscoelasticity*, first introduced by Levich [1962], on wave propagation has been studied extensively in both laboratory experiments [Hansen and Mann, 1964; Bock, 1987], and field experiments [Alpers and Hühnerfuss, 1989; Bock and Frew, 1993]. Evidence has recently been obtained that surface viscoelasticity affects not only the dissipation terms of the wave energy budget, but also the wind-wave growth and mixing terms [Bock *et al.*, 1995]. Results obtained in a small annular wind-wave tank at WHOI, described in a companion paper in this volume [Hara *et al.*, 1995], indicate a well-behaved functionality between mean square *wave slope* and gas-transfer coefficient for waves on clean water surfaces. Several studies have been performed in annular tanks at WHOI and at UH in order to understand how films of surface-active molecules influence both waves and gas transfer. Results from these studies show that even for different *surfactants* and concentrations, a uniform correlation between mean square slope and gas transfer is found. In view of the effect of the viscoelastic modulus on the wave field, the dependence of  $k$  on the viscoelastic modulus has also been investigated and the initial results of these studies are reported here.

## 2 Experimental Methods

Measurements of  $k$  were carried out in very clean water and in dilute aqueous solutions of a synthetic surfactant (*Triton-X-100*, polyethylene glycol p-tert-octylphenyl ether, avg. mol. wt 628, ®Rohm and Haas, Philadelphia, PA) in two annular wind-wave tanks of different scales at WHOI and UH. The WHOI tank has a mean diameter of 0.5 m and is designed to be relatively free of surface-active contaminants. The UH tank has a mean diameter of 4 m and is capable of sustaining longer waves. Due to its size, the UH tank is more difficult to keep free of adventitious surfactants and requires more aggressive removal of contaminant films through the continuous use of a surface skimming device.

Gas transfer velocities were measured during evasion or invasion experiments using primarily *oxygen* as a gas tracer.  $O_2$  measurements were made continuously using polarographic electrodes. *Sulfur hexafluoride* ( $SF_6$ ) was

also measured in selected experiments in the UH tank. Aqueous concentrations of SF<sub>6</sub> in discrete samples were measured by gas chromatography with electron capture detection.

Wind speed in the WHOI tank was taken nominally to be the mid-channel speed of the wind generating rotor; an anemometer was used to measure  $u$  in the larger UH tank. Since an accurate knowledge of the wind stress was essential for interpretation of the effects of surfactant films, friction velocities were measured for all experiments in both wind-wave tanks. A hot-film anemometer probe was used to measure bulk velocity profiles in the liquid phase in the UH tank; similar measurements were made in the WHOI tank using a Sontek acoustic current meter. A relation for estimating the water-side *friction velocity*  $u^*$  from bulk fluid velocity  $u_b$  ( $u^{*2} = u_b^2/\beta'$ ) was determined using the momentum balance method [Jähne *et al.*, 1987]. The drag coefficient  $\beta'$  was found to be relatively constant, except at low surface stress, where a transition from laminar to turbulent flow occurs.

Triton concentrations were varied from  $0.03 - 2.0 \times 10^{-6}$  mol  $\ell^{-1}$  to provide a range of viscoelasticities. Since liquid phase volumes for the UH tank were known only approximately and losses occurred during surface skimming, water samples were collected at the beginning and end of each experiment for determination of Triton concentrations. These were determined by solvent extraction of sample aliquots and measurement of the concentration using gas chromatography.

Wave propagation in subsamples of the same water was studied simultaneously in a small linear tank. Estimates of wave damping coefficients were made by measuring the propagation characteristics of mechanically generated wave packets at a frequency of 28.0 Hz. A point laser slope gauge positioned at known distances from the wavemaker was used to determine wave amplitude and phase. The frequency dependence of the damping coefficient allowed determination of the viscoelastic modulus using a dispersion relation incorporating viscoelasticity.

### 3 Results and Discussion

#### 3.1 Gas Transfer With Zero Viscoelastic Modulus

An objective of this study was to quantify the effects of synthetic surfactant films on gas transfer, which requires carefully controlled surface conditions. Experiments that are completely free of surfactant effects are difficult to achieve without extreme measures that unfortunately would be impractical for wind-wave tanks. Distilled waters typically contain significant amounts of surface-active organics that adsorb at the air-water interface. The presence of such adsorbable contaminants is reflected in a time-dependent decrease of wave slope and of mass transfer. Initial skimming of the surface only temporarily removes adsorbed films, which can quickly redevelop when skimming is discontinued. The experiments in the WHOI tank utilized

a commercially bottled spring water that, although not totally surfactant-free, contained very low amounts of organics and was significantly cleaner than the distilled water available in our laboratory. This allowed stable measurements over a period of hours. Filtered deionized water was used in the UH tank; initial experiments indicated that surface contamination developed within a short time of the initial skimming; therefore a skimmer was used continuously to remove adventitious surfactants and maintain relatively stable surface conditions.

Gas transfer velocities measured for different water surfaces in the WHOI tank are summarized in Figures 1-3. In Figure 1,  $k$  is shown to be a smooth function of wind speed in the case of the clean spring water surfaces, for which the viscoelasticity is expected to be negligible. Figure 2 shows the relation obtained between  $k$  and  $u^*$ . The transfer velocity increases as a smooth linear function of friction velocity. There is no pronounced transition from a smooth to wavy surface; waves were generally observed over the entire range of wind stress in the WHOI tank. A more stringent test for contaminants is to plot  $k$  normalized to  $u^*$  ( $k^* = k/u^*$ ) as shown in Figure 3. Within experimental error,  $k^*$  is constant for  $0.1 < u^* < 3.0 \text{ cm s}^{-1}$  in the clean case. This indicates that the near surface hydrodynamic regime was constant. Clean surface values for  $k^*$  measured in the UH tank are also plotted in Figure 3. For higher  $u^*$ , the UH clean water values are in close agreement with the WHOI values, suggesting that the scale of the tank is not a critical factor in comparing these measurements. At low to moderate  $u^*$ , the  $k^*$  values are suppressed relative to the WHOI values. This would be consistent with higher levels of organic matter in the water or from tank construction materials.

### 3.2 Gas Transfer With Non-Zero Viscoelastic Modulus

Transfer velocities were measured as a function of  $u^*$  for solutions of Triton at four different concentrations in the WHOI tank and three nominal concentrations in the UH tank; the latter varied from the nominal values due to depletions occurring during the measurements. Concentrations reported here are actual concentrations, measured as described in Section 2. Results for the WHOI tank are summarized in Figures 1-3. The observations for the UH tank were very similar and are included in Figures 3. Gas exchange was inhibited relative to clean water even for the lowest concentration measured ( $3 \times 10^{-8} \text{ mol } \ell^{-1} \text{ Triton}$ ). In the presence of Triton,  $k$  increased more slowly and nonlinearly with increasing wind speed (Figure 1) and also with  $u^*$  (Figure 2). The relation between  $u$  and  $k$  becomes increasingly nonlinear with increasing surfactant concentration and is qualitatively very similar to results reported by *Asher and Pankow* [1986; 1991] for gas transfer in stirred grid turbulent systems and to the Liss-Merlivat multilinear parameterization of  $k$  with wind for in situ gas exchange in lakes and seas [*Liss and Merlivat*, 1986]. A critical wind speed necessary for development of waves becomes apparent,

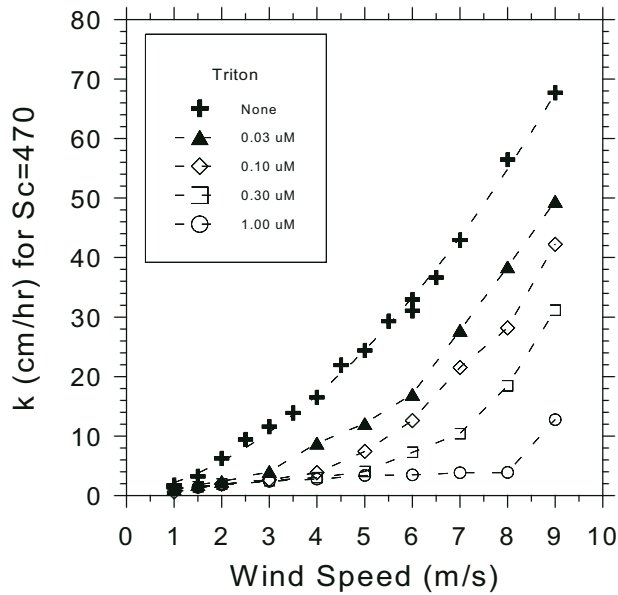


Figure 1: Dependence of gas transfer velocity,  $k$ , on wind speed,  $u$ , in the WHOI annular tank for clean water and dilute solutions of Triton-X-100.

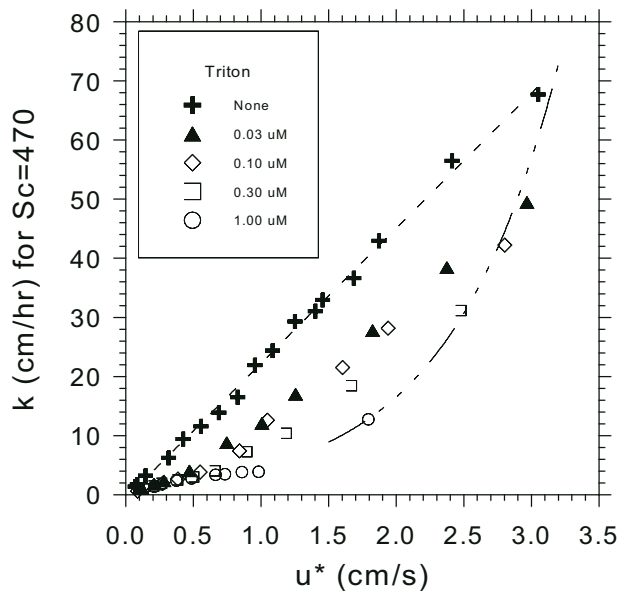


Figure 2: Gas transfer velocity as a function of water-side friction velocity,  $u^*$ , for clean water surfaces and for surfaces modified by different concentrations of Triton-X-100.

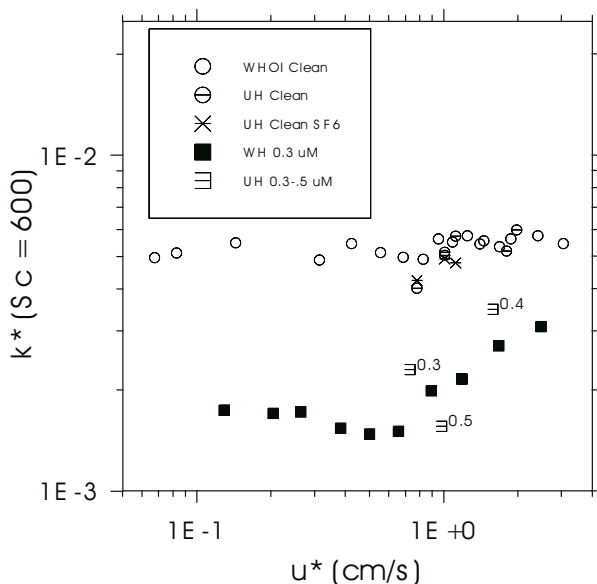


Figure 3: Dimensionless gas transfer coefficient,  $k^*$ , versus  $u^*$  for both clean water systems and for different concentrations of Triton-X-100. Data shown are from both WHOI and UH wind-wave facilities.

representing a transition between two hydrodynamic regimes. The *critical wind speed* increases with Triton-X-100 concentration. The inhibition of exchange is effective at the highest wind stress measured in the small tank ( $u^* = 3 \text{ cm s}^{-1}$ ). Comparison of Figures 1 and 2 illustrates the striking effect of surfactants on the drag presented by the interface. The broken line curve in Figure 2 is fitted to  $k$  values for  $u = 9 \text{ m/s}$ . At a concentration of  $1 \mu\text{mol } \ell^{-1}$ ,  $u^*$  is reduced to about 60% of the clean water value.

The transfer velocity can be expressed in terms of  $u^*$  as the dimensionless transfer velocity  $k^* = k/u^* = \beta Sc^{-n}$ . In Figure 3, the variation of  $k^*$  with  $u^*$  for a Triton solution ( $0.3 \mu\text{mol } \ell^{-1}$ ) is compared with  $k^*$  values for clean water for the WHOI tank, along with data for similar concentrations in the UH facility. These have been normalized to  $Sc = 600$  by assuming Schmidt number dependencies of  $n = 1/2$  for wavy surfaces and  $n = 2/3$  for smooth surfaces. However, the Schmidt number exponent is likely to have intermediate average values in the transition region, as shown by correlations of  $n$  with wave slope and by direct measurements of  $n$  using multiple gas tracers [Jähne *et al.*, 1987].

In contrast to the clean water values,  $k^*$  is strongly suppressed at low  $u^*$  and does not attain clean water values even at high  $u^*$ . A clear transition between hydrodynamic regimes (smooth surface to wavy surface) is observed. This transition occurred at different  $u^*$  for different surfactant

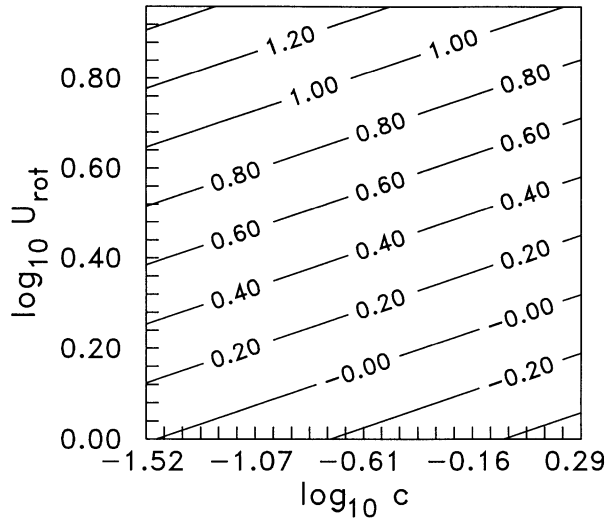


Figure 4: Surface contour plot of  $\log_{10} k$  as a function of  $\log_{10} c$  and  $\log_{10} u_{rot}$ . Data points represent measurements from both the WHOI and UH facilities. A planar surface fitted by means of least-squares-fit is depicted in the contour plot and explains the variance of 90% of the data.

concentrations.

As with surfactants that occur in natural waters [Frew and Nelson, 1992a; 1992b; Bock and Frew, 1993], Triton-X-100 is water-soluble, but forms films that are not reversibly adsorbed and desorbed at the interface. When Triton-X-100 films were allowed to accumulate in the absence of surface skimming, increased suppression of exchange was observed at a given surfactant concentration. Under conditions of constant surface skimming, the surface concentration of Triton-X-100 was expected to be in dynamic equilibrium with the bulk concentration,  $c$ , through diffusional exchange. Figure 4 shows the fitted three-dimensional plane that describes the  $\log_{10} c$ - $\log_{10} u$ - $\log_{10} k$  relation that describes the experimental data for both the WHOI and UH wind-wave tanks. The plane describes within one standard deviation, the variance in 90% of the data points.

The results suggest that the Triton, a highly water-soluble surfactant, was capable of maintaining significant viscoelasticity at the interface despite the continuous disruption of the surface by the skimming device, which prevented accumulation of film material. This finding implies that natural soluble surfactants in seawater also could affect gas transfer under conditions where films of water-insoluble surfactants would be disrupted by wind shear and breaking waves.

### 3.3 Estimation of Wave Damping and Viscoelastic Modulus

A strong linear correlation between  $k$  and *mean squared surface slope* was observed for clean interfaces [Hara *et al.*, 1995]. The same relationship was also observed to apply in the presence of Triton-X-100. Apparently the surface roughness is an indicator of the turbulence phenomena governing the exchange. A study of the wave damping effects of the Triton was undertaken to try to correlate damping coefficients and  $k$ . An analysis of the data obtained from these experiments yielded values of the viscoelastic modulus.

Levich [1962] established early that the presence of a surface dilational elasticity caused damping of capillary and *capillary-gravity waves* by creating a surface tension gradient due to wave orbital motion. The hydrodynamic description was re-evaluated by Bock and Mann [1989] to eliminate spurious wave propagation modes and the resulting *dispersion relation* was formulated from the linearized Navier-Stokes relation and surface boundary conditions that include a dilational visco-elastic modulus. This dispersion relation is limited in the sense that surface shear viscoelasticity and other more complex surface rheological properties are omitted. Despite this, the formulated dispersion relation should be accurate for dilute gas-like surface films where shear viscoelasticities and surface plasticity should not exist. It relates the physical properties of the bulk fluid on which the waves propagate (namely the density,  $\rho$ , and the fluid viscosity,  $\eta$ ), along with the *surface tension*,  $\sigma$ , and the gravitational constant,  $g$ , to waves with angular frequency,  $\omega$ , that have a complex wavenumber,  $\hat{k}$ , that is defined as:

$$\hat{k} = \frac{2\pi}{\lambda} + i\beta \quad (1)$$

where  $\lambda$  is the wavelength of the wave and  $\beta$  is the distance damping coefficient. The dispersion relation takes the form of a determinant that is equal to zero when values of  $\hat{k}$  and  $\omega$  are obtained that satisfy physically realistic wave propagation. The relation is given as:

$$\begin{vmatrix} (\rho\omega^2 - \rho g\hat{l} + 2i\omega\eta\hat{l}^2 - \sigma\hat{k}^2\hat{l}) & (-i\rho g\hat{k} - 2\omega\eta\hat{m}\hat{k} - i\sigma\hat{k}^3) \\ (2\omega\eta\hat{k}\hat{l} + i\hat{e}\hat{k}^3) & (i\omega\eta[\hat{k}^2 + \hat{m}^2] - \hat{e}\hat{k}2\hat{m}) \end{vmatrix} = 0 \quad (2)$$

where  $\hat{m}$  is defined as:

$$\hat{m} = +\sqrt{\hat{k}^2 - \frac{i\omega\rho}{\eta}} \quad (3)$$

and  $\hat{l}$  is defined as:

$$\hat{l} = +\sqrt{\hat{k}^2} \quad (4)$$

This dispersion relation predicts wave modes that correspond to the Laplace mode in which the primary restoring force for wave motion is the surface tension acting on the curvature of the wave. In the presence of a surface dilational viscoelasticity, a Marangoni mode is predicted, along with a modified Laplace mode. In this mode the primary restoring force is produced by local areas of compressed surface film that give rise to an oscillating compressional wave in the plane of the surface.

The dispersion relation can be solved to obtain the *viscoelastic modulus*,  $\hat{\epsilon}$  by using experimentally obtained values for the remaining variables. To obtain the real and imaginary parts of  $\hat{k}$ , plane-wave packets are produced at the end of a 1.3 m linear wave tank. The packets propagate along the tank and a single-point slope gauge, that can be positioned at known locations along the tank, records its passage. Figure 5 shows a representative time series recorded at a point along the tank. Measurement of the phase of the wave packet at several 0.001 m spacings gives an accurate estimate of the real part of  $\hat{k}$ , and measurements of the packet amplitude at 0.05 m intervals give an estimate of the imaginary part,  $\beta$ . Separate measurement of surface tension is performed using a Wilhelmy plate and an electrobalance. Having experimentally fixed the frequency of the wave and using tabulated values for density, viscosity, and the gravitational constant, it is possible to solve iteratively the dispersion relation for  $\hat{\epsilon}$ . It is also possible to solve the dispersion relation assuming that the viscoelastic modulus is zero, corresponding to waves propagating on a clean surface with no surface film. This allows computation of  $\beta_E/\beta_T$ , the *damping ratio*,  $R$ .

For the wave damping experiments, three concentrations of Triton were tested. These concentrations were 0.01, 0.03, and 0.3  $\mu\text{M}$ . The wave packet frequency was centered at 28.0 Hz, the density, viscosity, and gravitational constant used for the calculations were 0.998  $\text{g}/\text{cm}^3$ , 0.01 P, and 981  $\text{cm}/\text{s}^2$ , respectively. Because the results of these experiments were to be compared with the gas transfer measurements described above, it was important to create surface conditions in the linear tank that corresponded to the conditions in the annular wind-wave tank. Intrinsically, this could not be achieved because the quiescent conditions required for mechanically generated waves in the linear tank are not the same as the mixed, dynamical conditions obtained with wind stress generated over the surface in the annular tank. To simulate the effect that mixing would produce in the wind-wave tank, the surface of the linear tank was aspirated at one end while being re-supplied at the other end with a stream of solution of the same concentration in the tank. This process removed the very surface of the solution (and also incidentally caused a small surface drift) that resulted in a surface free of a statically adsorbed film. At the instant of the start of the wave measurements, the aspiration and re-supply were ended, and the surfactant was allowed to adsorb at its own pace. The surface tension was observed to decrease monotonically, indicating the re-adsorption of surfactant. While this took place, measurements proceeded at intervals of 10 minutes so that the

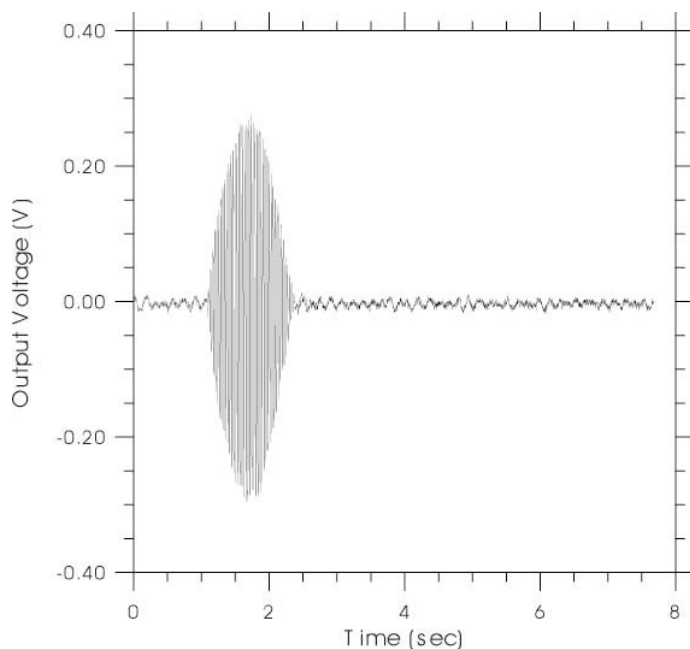


Figure 5: Representative wave packet from a 28 Hz wave produced in the linear wave tank. These data represent the time history of surface slope as observed at a fixed distance away from the mechanical wave generator.

calculated  $\hat{\epsilon}$  and  $\beta_E/\beta_T$  values could be obtained. These values would then be extrapolated back in time to the start of the experiment to yield values representative of a fresh surface.

Results of these experiments were amplitude and phase versus distance at discrete points in time after the start of the experiment. In Figure 6, points are plotted representing packet amplitude as a function of distance away from the wave maker. Each of the lines represents a measurement made in 10 minute intervals from the start of the experiment. It is clear that the slope of these lines increases, indicating a larger value of distance damping coefficient. A similar phenomenon is demonstrated in the wavenumber ( $2\pi/\lambda$ ), as a function of time. This evidence, along with the steady decrease in surface tension demonstrates how the surface of the solution ages. While it is not clear that the surface of the solution in the wind-wave tank is as efficiently stripped of a static adsorbed film under the conditions of wind-stress during a gas exchange measurement, we do not have the means to measure mechanically generated waves in the wind-wave tank.

The results in Table 1 include both measured and calculated properties for three different solutions of Triton-X-100. As stated above, these parameters are determined after thorough surface aspiration. Since the surface is initially stripped of adsorbed films, the initial surface tension,  $\sigma_0$  is close

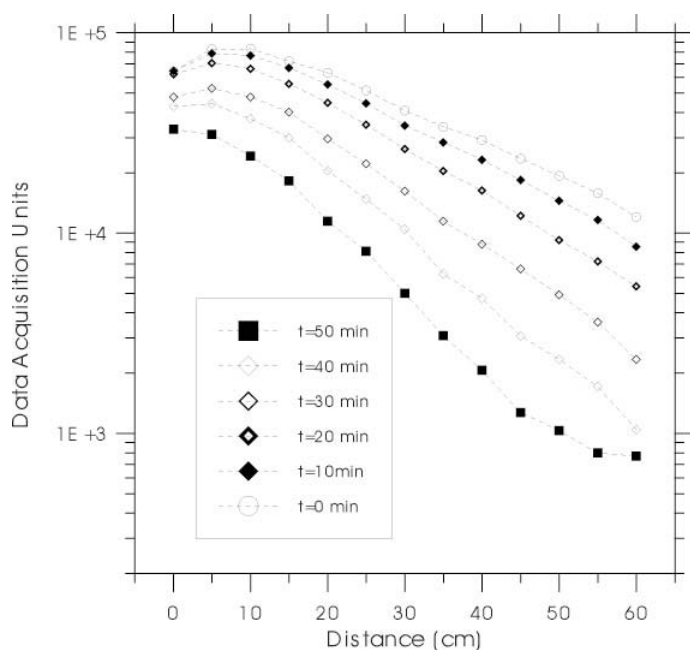


Figure 6: Damping curves (log amplitude versus distance) for wave packets at 28 Hz. The waves are propagating on a solution of  $0.3 \mu\text{M}$  Triton-X-100. As the surface film adsorbs, the wave propagation is modified and the distance damping coefficient increases.

to that of pure water. For this reason, the theoretical wavenumber (calculated from the dispersion relationship with zero viscoelasticity) does not significantly vary with Triton concentration. For the  $0.03 \mu\text{M}$  solution, the measured damping coefficient was not significantly different from the theoretical damping coefficient. Although small, the measured damping coefficient for the  $0.1 \mu\text{M}$  solution was found to increase from the theoretical value. A much larger increase in the damping coefficient was measured for the  $0.30 \mu\text{M}$  solution. A similar trend in the elasticity was observed. The uncertainty pertaining to the elasticity in the  $0.03 \mu\text{M}$  solution was of the same order as the value itself. However, the  $0.1 \mu\text{M}$  and  $0.3 \mu\text{M}$  showed appreciable increases in elasticity. In all cases, the imaginary part of the viscoelasticity was negligible. This was probably due, in part, to the slow adsorption of Triton-X-100 at this concentration.

Comparison with the data in Figure 1 indicates that both  $R$  and  $\epsilon_d$  are inversely correlated with  $k$  for a given  $u$ . However, the ability to correlate the wave damping characteristics and viscoelasticity with the gas transfer results is complicated by the ability to reproduce the same surface in separate experiments. This is a strong disadvantage of using Triton-X-100 and similar surfactants, that other researchers should be aware of. With the same

*Table 1: Summary of wave damping and viscoelastic modulus*

Concentration	0.03 $\mu\text{M}$	0.10 $\mu\text{M}$	0.30 $\mu\text{M}$
$\sigma_0$ (mN/m)	72.56	72.13	72.16
$k_T$ (rad/cm)	6.9312	6.9456	6.9482
$k_E$ (rad/cm)	6.9407	6.9177	6.6394
$\beta_T$ (1/cm)	.02848	.02866	.02870
$\beta_E$ (1/cm)	.02823	.02939	.03571
$R$	0.9912	1.0255	1.3425
$\epsilon_d$ (mN/m)	-0.3974	0.8709	2.7290
$\eta_d$ (g/s)	-1.3E-4	1.1E-3	7.5E-3

bulk concentrations of absorbed surface active material, the actual surface concentration may vary substantially. This depends on many conditions which are difficult to control. If the surface is not continuously stripped of adsorbed films, the surface concentration will increase and both the damping coefficient and the viscoelasticity will also increase. There does remain a strong correlation between gas transfer velocity and bulk concentration. The results of this preliminary study indicate that the degree of the inverse relationship of gas transfer velocity and concentration may be determined by the surface viscoelasticity and the damping coefficient.

## 4 Concluding Remarks

Excellent agreement was obtained between the WHOI and UH facilities for determination of gas transfer velocity as a function of wind-stress. As expected, significant reduction of the gas transfer velocity was effected by surfactant films. A three-way power-law relation is seen in the data, which suggest a simple relation between gas transfer velocity, Triton-X-100 concentration, and wind. While it is not intuitive that concentration should form a simple relation to gas transfer velocity, there exists a strong inverse correlation between wave damping enhancement and gas transfer velocity.

## Acknowledgements

The authors thank R. K. Nelson for his determinations of Triton-X-100 in the samples used, and C. G. Johnson, T. Donahue and J. Ledwell for their advice and assistance in developing the  $\text{SF}_6$  gas chromatographic technique used at UH. This research was supported by the National Science Foundation under grants OCE-9301334 and OCE-9410537. Contribution No. 9071 of the Woods Hole Oceanographic Institution.

## References

- Alpers, W. and H. Hühnerfuss, The damping of ocean waves by surface films: a new look at an old problem. *J. Geophys. Res.*, 94, 6251–6265, 1989
- Asher, W. E. and J. F. Pankow, The interaction of mechanically generated turbulence and interfacial films with a liquid phase controlled gas/liquid transport process. *Tellus*, 38B, 305–318, 1986
- Asher, W. E. and J. F. Pankow, The effect of surface films on concentration fluctuations close to a gas/liquid interface. In *Air-Water Mass Transfer*, S. C. Wilhelms and J. S. Gulliver eds, (pp.68–79): New York: American Society of Civil Engineers, 1991
- Bock, E. J., On ripple dynamics. I. Microcomputer-aided measurement of ripple propagation. *J. Colloid Interfac. Sci.*, 119, 326–33, 1987
- Bock, E. J., T. Hara and M. Donelan, Equilibrium spectra of wind waves in the presence of surfactants (in preparation)
- Bock, E. J. and N. M. Frew, Static and dynamic response of natural multicomponent oceanic surface films to compression and dilation: laboratory and field observations. *J. Geophys. Res.*, 98, 14599–14617, 1993
- Davies, J. T., The effects of surface films in damping eddies at a free surface of a turbulent liquid. Proceedings of the Royal Society of London, A290, 515–526, 1966
- Frew, N. M., The role of organic films in air-sea gas exchange. In: *The Sea Surface and Global Change*, P. S. Liss and R. A. Duce, eds., Cambridge University Press, 1995 (in press)
- Frew, N. M. and R. K. Nelson, Isolation of marine microlayer film surfactants for ex situ study of their surface physical and chemical properties. *J. Geophys. Res.*, 97, 5281–5290, 1992a
- Frew, N. M. and R. K. Nelson, Scaling of marine microlayer film surface pressure-area isotherms using chemical attributes. *J. Geophys. Res.*, 97, 5291–5300, 1992b
- Hansen, R. S. and J. A. Mann Jr., Propagation characteristics of capillary ripples. I. The theory of velocity dispersion and amplitude attenuation of plane capillary waves on viscoelastic films. *J. Appl. Phys.*, 35, 152–161, 1964
- Hara, T., E. J. Bock, N. M. Frew, and W. R. McGillis, Relationship between air-sea gas transfer velocity and surface roughness, *This volume*
- Jähne, B., O. Münnich, R. Bösinger, A. Dutzi, W. Huber and P. Libner, On the parameters influencing air-water gas exchange. *J. Geophys. Res.*, 92, 1937–1949, 1987
- Lee, Y. H., G. T. Tsao and P. C. Wankat, Hydrodynamic effect of surfactants on gas-liquid oxygen transfer. *AIChE Journal*, 26, 1008–1012, 1980
- Levich, V. G., [1962] *Physico-Chemical Hydrodynamics*. Englewood Cliffs, NJ: Prentice Hall, 1962
- Liss, P. S. and L. Merlivat, Air-sea gas exchange rates: introduction and synthesis, in *The Role of Air-Sea Exchange in Geochemical Cycling* (P. Buat-Menard ed.), Reidel, Dordrecht, pp. 113–127, 1986
- Wanninkhof, R., Relationship between wind speed and gas exchange over the ocean. *J. Geophys. Res.*, 97, 7373–7382